An integrated optic ethanol vapor sensor based on a silicon-on-insulator microring resonator coated with a porous ZnO film

Nebiyu A. Yebo,[1,*] Petra Lommens,[2] Zeger Hens,[2] and Roel Baets[1]

[1]*Ghent University-IMEC, Photonics Research Group, INTEC, Sint-Pietersnieuwstraat 41, 9000 Gent, Belgium*
[2]*Ghent University, Physics and Chemistry of Nanostructures, Krijgslaan 281-S3, 9000 Gent, Belgium*
**nyebo@intec.ugent.be*

Abstract: Optical structures fabricated on silicon-on-insulator technology provide a convenient platform for the implementation of highly compact, versatile and low cost devices. In this work, we demonstrate the promise of this technology for integrated low power and low cost optical gas sensing. A room temperature ethanol vapor sensor is demonstrated using a ZnO nanoparticle film as a coating on an SOI micro-ring resonator of 5 µm in radius. The local coating on the ring resonators is prepared from colloidal suspensions of ZnO nanoparticles of around 3 nm diameter. The porous nature of the coating provides a large surface area for gas adsorption. The ZnO refractive index change upon vapor adsorption shifts the microring resonance through evanescent field interaction. Ethanol vapor concentrations down to 100 ppm are detected with this sensing configuration and a detection limit below 25 ppm is estimated.

OCIS codes: (130.6010) Sensors; (280.4788) Optical sensors and sensing.

References and links

1. A. Airoudj, D. Debarnot, B. Bêche, and F. Poncin-Epaillard, "Design and sensing properties of an integrated optical gas sensor based on a multilayer structure," Anal. Chem. **80**(23), 9188–9194 (2008).
2. M. El-Sherif, L. Bansal, and J. Yuan, "Fiber optic sensors for detection of toxic and biological threats," Sensors **7**(12), 3100–3118 (2007).
3. B. Timmer, W. Olthuis, and A. Berg, "Ammonia sensors and their applications- a review," Sens. Actuators B Chem. **107**(2), 666–677 (2005).
4. I. Syhan, A. Helwig, T. Becker, G. Muller, I. Elmi, S. Zampolli, M. Padilla, and S. M. Marco, "Discontinuously operated metal oxide gas sensors for flexible tag microlab applications," IEEE Sens. J. **8**(2), 176–181 (2008).
5. S. M. Kanan, O. M. El-Kadri, I. A. Abu-Yousef, and M. C. Kanan, "Semiconducting metal oxide based sensors for selective gas pollutant detection," Sensors **9**(10), 8158–8196 (2009).
6. X. L. Cheng, H. Zhao, L. H. Huo, S. Gao, and J. G. Zhao, "ZnO nanoparticulate thin film: preparation, characterization and gas-sensing properties," Sens. Actuators **102**(2), 248–252 (2004).
7. A. Forleo, L. Francioso, S. Capone, P. Siciliano, P. Lommens, and Z. Hens, "Synthesis and gas sensing properties of ZnO quantum dots," Sens. Actuators B Chem. **146**(1), 111–115 (2010).
8. P. Dumon, W. Boagerts, A. Tchelnokov, J.-M. Fedili, and R. Baets, "Silicon nanophotonics," Future Fab. International **25**, 29–36 (2008).
9. N. Jokerst, M. Royal, S. Palit, L. Luan, S. Dhar, and T. Tyler, "Chip scale integrated microresonator sensing systems," J Biophotonics **2**(4), 212–226 (2009).
10. Y. Sun, and X. Fan, "Analysis of ring resonators for chemical vapor sensor development," Opt. Express **16**(14), 10254–10268 (2008).
11. N. Yebo, D. Taillaert, J. Roels, D. Lahem, M. Debliquy, D. van Thourhout, and R. Baets, "Silicon-on-insulator (SOI) ring resonator based integrated optical hydrogen sensor," IEEE Photon. Technol. Lett. **21**(14), 960–962 (2009).
12. A. Nitkowski, L. Chen, and M. Lipson, "Cavity-enhanced on-chip absorption spectroscopy using microring resonators," Opt. Express **16**(16), 11930–11936 (2008).
13. J. T. Robinson, L. Chen, and M. Lipson, "On-chip gas detection in silicon optical microcavities," Opt. Express **16**(6), 4296–4301 (2008).
14. T. Claes, J. G. Molera, K. De Vos, E. Schacht, R. Baets, and P. Bienstman, "Label-free biosensing with a slot – waveguide-based ring resonator in silicon on insulator," IEEE Photonics J. **1**(3), 197–204 (2009).

#126035 - $15.00 USD Received 26 Mar 2010; revised 5 May 2010; accepted 7 May 2010; published 20 May 2010

15. F. Y. Gardes, A. Brimont, P. Sanchis, G. Rasigade, D. Marris-Morini, L. O'Faolain, F. Dong, J. M. Fedeli, P. Dumon, L. Vivien, T. F. Krauss, G. T. Reed, and J. Martí, "High-speed modulation of a compact silicon ring resonator based on a reverse-biased pn diode," Opt. Express **17**(24), 21986–21991 (2009).
16. P. Dumon, W. Bogaerts, V. Wiaux, J. Wouters, S. Beckx, J. Van Campenhout, D. Taillaert, B. Luyssaert, P. Bienstman, D. Van Thourhout, and R. Baets, "Low-loss SOI photonic wires and ring resonators fabricated with deep UV lithography," IEEE Photon. Technol. Lett. **16**(5), 1328–1330 (2004).
17. B. J. Melde, B. J. Johnson, and P. T. Charles, "Mesoporous silicate materials in sensing," Sensors **8**(8), 5202–5228 (2008).
18. J. Kobler, and T. Bein, "Porous thin films of functionalized mesoporous silica nanoparticles," ACS Nano **2**(11), 2324–2330 (2008).
19. M. R. Baklanov, K. P. Mogilnikov, V. G. Polovinkin, and F. N. Dultsev, "Determination of pore size distribution in thin films by ellipsometric porosimetry," J. Vac. Sci. Technol. B **18**(3), 1385–1391 (2000).
20. S. K. Selvaraja, P. Jaenen, W. Bogaerts, D. Van Thourhout, P. Dumon, and R. Baets, "Fabrication of photonic wire and crystal circuits in silicon-on-insulator using 193nm optical lithography," J. Lightwave Technol. **27**(18), 4076–4083 (2009).
21. D. A. Schwartz, N. S. Norberg, Q. P. Nguyen, J. M. Parker, and D. R. Gamelin, "Magnetic quantum dots: synthesis, spectroscopy, and magnetism of Co^{2+} - and Ni^{2+}-doped ZnO nanocrystals," J. Am. Chem. Soc. **125**(43), 13205–13218 (2003).
22. P. Lommens, D. Van Thourhout, P. F. Smet, D. Poelman, and Z. Hens, "Electrophoretic deposition of ZnO nanoparticles: from micropatterns to substrate coverage," Nanotechnology **19**(24), 245301 (2008).
23. Y. Wang, Z. Zhou, Z. Yang, X. Chen, D. Xu, and Y. Zhang, "Gas sensors based on deposited single-walled carbon nanotube networks for DMMP detection," Nanotechnology **20**(34), 345502 (2009).
24. P. Atkins, and J. de Paula, Atkins, *Physical Chemistry 7th ed.* (Oxford Univ. Press, 2002).

1. Introduction

Gas detection is a vital element in several industrial, medical and environmental applications, like environmental pollution monitoring, industrial process monitoring, leak detection of explosive gases, and medical breath analysis. A trend in current sensor development is miniaturization to obtain inexpensive and compact gas sensors that are robust and safe, have low power consumption and enable multiplexing of sensor arrays and remote sensing [1–3]. Furthermore, miniaturization opens a way to a chip level implementation, integration with other vital functionalities, and mass fabrication.

Gas sensors developed for miniaturization use various detection principles, like electrochemical, catalytic or optical detection [1,3]. A widely used sensor concept is electrochemical sensing using the change of resistance of metal oxide semiconductors (MOS) upon gas adsorption [3–7]. However, MOS sensors often require operation at elevated temperature to achieve higher sensitivities. Therefore, high power consumption has been an issue with such sensors [4]. In addition, the sparking risks associated with the electrical contacts further make these sensors potentially unsafe for operation in explosive environments. Optical gas sensors have the potential to solve these problems. They can be operated at room temperature and often require no electrical connections [1]. So far, optical sensing has been dominantly achieved by means of optical fibers [1,2]. This, however, is an approach that does not readily lend itself for miniaturization and integration.

Silicon on Insulator (SOI) was recently proved to be a viable technology for a wide range of integrated optical applications [8–13]. Photonic SOI structures have been demonstrated with submicron scale features and can be realized on a very small area on a chip due to the high index contrast between the waveguides and the surrounding claddings. Moreover, the compatibility of the SOI devices with CMOS fabrication tools and the promise of inexpensive mass fabrication makes them highly attractive. Owing to these facts, the research on SOI optical structures is recently extending beyond telecom to other applications such as optical bio-molecule and gas sensing [8–13].

Here, we explore optical gas sensing by coating an SOI microring resonator (MRR) with a porous film of ZnO nanocrystals. Using transducer chemical coatings on optical circuits is not uncommon in optical sensing [1,2] since they strongly reduce the interaction length as compared to a direct spectroscopic gas analysis. Moreover, a proper choice of both the sensitive optical component and the chemical coating can lead to a significant enhancement in the sensor response. Chemical coatings made from metal oxides as used here have been extensively studied for electrical gas sensing applications [3–7], but not so much for optical

#126035 - $15.00 USD Received 26 Mar 2010; revised 5 May 2010; accepted 7 May 2010; published 20 May 2010

gas sensing. Using a ZnO coated MRR, we show the detection of 100 ppm ethanol in air at room temperature and predict a detection limit below 25 ppm. This result demonstrates the promise of a reasonably sensitive, compact and inexpensive optical gas sensors based on SOI technology.

2. Porous sensitive films on micro ring resonators for gas sensing

MRRs, as shown in the SEM image in Fig. 1(a), are optical circuits in which light propagates as circulating waveguide modes [10], provided that an integer times the wavelength λ matches the product of the guided mode effective refractive index n_{eff} and the physical length L of the resonator:

$$n\lambda = n_{eff}(n_S, \lambda) \times L. \tag{1}$$

Equation (1) stresses the fact that n_{eff} depends both on the refractive index n_s of the surrounding medium and on the wavelength. This implies that any change in the surrounding medium that affects n_{eff} can be measured through the resulting resonance shift of the MRRs. Introducing the group index n_g of the guided mode, one readily demonstrates that the resonance shift $\Delta\lambda$ associated to a small change Δn_s can be expressed as [14–16]:

$$\frac{\Delta\lambda}{\lambda} = \left.\frac{\partial n_{eff}}{\partial n_s}\right|_{\lambda} \frac{\Delta n_s}{n_g}. \tag{2}$$

As a result, MRRs fabricated on SOI technology have recently been explored for highly compact integrated optical sensing applications [9–13]. They have inherent features suitable for compact sensor implementation. First, any change in the surrounding medium that affects n_{eff} can be measured through the resonance shift $\Delta\lambda$ of the MRR. This provides a multiplexing capability and less sensitivity to input power noise. Second, due to the repeated light circulation at the resonance wavelengths, high sensitivity to the surrounding physical changes can readily be achieved even for rings as small as 5μm in radius [11].

More precisely, the sensitivity and the detection limit of MRR based sensors depend on the quality factor Q and the confinement factor Γ of the MRR. High Q ring resonators have longer effective lengths due to the reduced propagation losses. This raises the effective interaction length with the surroundings, leading to an increase in sensitivity. Moreover the minimum measurable or resolvable resonance shift, which determines the detection limit, is improved for high Q MRRs. The SOI MRRs used in this work have Q values of about 15000 after coating with ZnO nanocrystals. The other important factor, Γ, measures the magnitude of the evanescent field extending outside the waveguides for the interaction with the surrounding [10]. The effective interaction length, L_{eff} of a MRR depends on Q and Γ, where higher quality and confinement factors raise L_{eff} (Eq. (3) [12].

$$L_{eff} = \Gamma \frac{Q\lambda}{2\pi n_g}. \tag{3}$$

To detect the concentration of gas molecules in an environment, MRRs can be functionalized by sensitive chemical coatings. The physical changes in such sensitive coatings can modulate the MRR resonance in different ways. For example, n_{eff} is affected by a change in refractive index of the coating through evanescent field interaction, or by a temperature increase of the MRR caused by a chemical reaction initiated in the coating [9,11]. Of course, films of an adequate sensitivity are required to achieve detectable resonance shifts at low gas concentrations. In this respect, porous films have recently become attractive since they offer a large surface area for gas adsorption, resulting in a high sensitivity [17]. Mesoporous films

#126035 - $15.00 USD Received 26 Mar 2010; revised 5 May 2010; accepted 7 May 2010; published 20 May 2010

with pore sizes ranging from 2 to 50 nm, in particular, can provide surface areas as high as 1000 m^2/g [17,18].

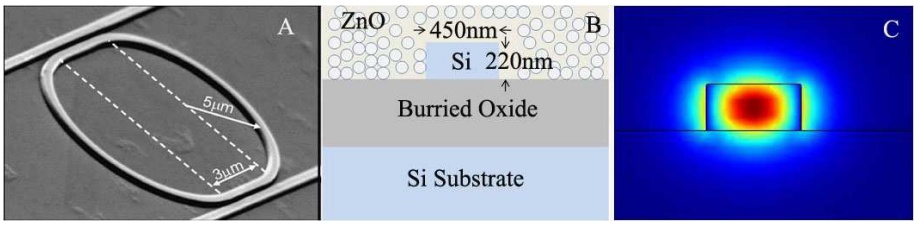

Fig. 1. (a) A scanning electron microscope (SEM) image of an SOI MRR of 5μm radius. (b) Cross section view of the SOI ethanol sensor structure. (c) TE mode electric field profile of a 450nm wide and 220nm high SOI waveguide with ZnO cladding, simulated with COMSOL Multiphysics.

In this work, we have coated MRRs with films of 3.5 nm ZnO nanocrystals for optical sensing of gaseous ethanol. ZnO is an attractive material in this respect due to its affinity to volatiles, low toxicity, convenience for doping, and low cost [6,7]. Moreover, ZnO is transparent in the near infrared around 1550 nm, enabling applications based on evanescent field interactions in SOI. Finally, literature results indicate that ZnO nanocrystalline films show a good electrical sensitivity to alcohols at lower operating temperatures [6,7].

Figure 1(b) show an impression of the cross section of the basic sensor structure of a MRR coated by a film of stacked nanocrystals. As these films are inherently porous, adsorption of ethanol by the ZnO nanocrystals may induce a MRR resonance wavelength shift due to evanescent field interaction. Using the Lorentz-Lorenz equation for a composite (porous) medium [19], we can estimate the refractive index of the ZnO coating. Assuming a porosity of 40% and a refractive index n_{ZnO} of 1.93, we obtain a value of 1.483. The resulting simulated electric field profile of the sensor structure, *i.e.*, a 450 nm wide and 220 nm high SOI waveguide coated with the ZnO film, is shown in Fig. 1(c). Following this field profile, a confinement factor of 0.23 is calculated in the porous coating at 1530 nm.

For a MRR evanescent wave sensor, Eq. (2) can be represented by Eq. (4), where the changes in mode effective index and the coating refractive index are directly related through Γ [13]:

$$\frac{\Delta\lambda}{\lambda} = \left.\frac{\partial n_{eff}}{\partial n_s}\right|_{\lambda} \frac{\Delta n_s}{n_g} = \Gamma \frac{\Delta n_{coating}}{n_g}. \qquad (4)$$

If we attribute the change in refractive index of the ZnO nanocrystal film upon adsorption to the partial filling of the pores by ethanol molecules, an estimate of the expected resonance wavelength shift can be obtained using once more the Lorentz-Lorenz equation. With a layer porosity of 40% and assuming that 10% of the pores are filled with ethanol (n = 1.35), a refractive index change of the film of about 0.0172 is obtained, corresponding to a change Δn_{eff} of 4 10^{-3}. With a group index of 4.96, calculated from the 15 nm free spectral range of the ZnO coated MRRs, this results in an MRR resonance shift of 1.2 nm at 1530 nm. Using the actual 50 pm half width at half maximum of the ring resonances as a detection limit, such shifts are readily detectable. Importantly, the small changes in n_{eff} ensure that the wavelength shift measured is directly proportional to the volume of ethanol adsorbed by the coating.

3. Sample Fabrication and Preparation

The MRRs with grating couplers have been fabricated with standard CMOS fabrication facilities. In practice, 193 nm deep UV photolithography in combination with dry etching is used to fabricate high Q (> 25000) resonators. The fabrication details are well documented in ref [16,20]. The ZnO nanoparticles are synthesized following a low temperature synthesis technique [21,22]. A 15 mL solution of 0.1 M, 99.99% pure zinc acetate in dimethyl sulfoxide

#126035 - $15.00 USD Received 26 Mar 2010; revised 5 May 2010; accepted 7 May 2010; published 20 May 2010

is vigorously stirred at room temperature and 5 mL of a 0.5 M solution of tetramethylammonium hydroxide (98% pure) in ethanol is added drop-wise over a time span of 10-15 min. The resulting ZnO nanoparticles are precipitated by adding 40 mL of ethyl acetate. After centrifugation (2000 rpm/2min), the supernatant containing most of the unreacted precursor salts is removed and the remaining nanoparticles are resuspended in 20 mL of ethanol. Afterwards, they are washed a second time by adding 40 mL of a 1:1 mixture of ethyl acetate and heptanes and again resuspended in 20 mL of ethanol to obtain a transparent and colorless suspension.

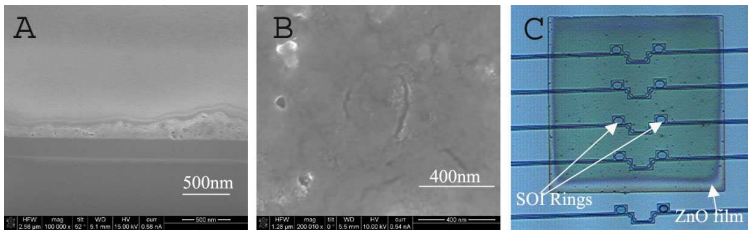

Fig. 2. (a) SEM cross section view of a drop casted ZnO film on an SOI sample. (b) SEM image showing the top view of the ZnO film. (c) Optical microscope image of a rectangular ZnO nanparticle coating covering four pairs of closely situated SOI MRRs, with an indication of the coating and the MRRs.

To facilitate the local deposition of ZnO nanocrystal films, negative photoresist (AZ 2070 from Micro chemicals) patterns are prepared on the SOI chip. This is done by a 365 nm Ultra Violet (UV) photolithographic process. The patterned sample is finally baked at 140 °C for 2 min to make the photoresist resistant to the ethanolic suspension [22]. To prepare sufficiently thick ZnO nanoparticle films, the nanoparticle suspension is drop cast on this patterned sample and allowed to dry in air for 15 min. Finally, lift-off of the photoresist is achieved by means of a 1-methylpyrrolidine solution at 80 °C, leaving porous local coatings around the ring resonators. Figure 2 shows the scanning electron microscope (SEM) and optical images of a roughly 200 nm thick ZnO film on MRRs. In spite of the non uniformity in film thickness and irregularities in morphology, the optical quality of these nanocrystal films is sufficient for the work envisaged here. Most likely, this is because the film is thick enough such that the evanescent field does not interact with the rough, non-uniform surface. If required, the coating procedure can be adapted in the future to make better quality films. After coating the ZnO film, the sample is heated at 100 °C for 2 min in order to make sure that all the ethanol (solvent) residue is removed.

4. Experimental results

The schematic in Fig. 3 shows the experimental setup. The ZnO coated SOI chip is placed in a gas chamber whose top side is sealed with a transparent glass window such that light can be coupled vertically through it. The chamber is kept at atmospheric pressure. A coupling fiber from a tunable laser (Santec TSL- 510) is aligned to the input grating couplers at 10 degrees from the vertical. The light from the output gratings is collected with an IR camera (XenIcs Xeva-511). Homemade software is used to control the laser and the camera, and to record the data.

Different concentrations of ethanol vapor are obtained by bubbling a small volume of liquid ethanol with air. The vapor concentrations at different temperatures are estimated using the Antoine equation [23]. The bubbler is kept at low temperature (0 °C) in order to lower the ethanol vapor pressure. The resulting saturated vapor is diluted with air at different flow rates to adjust the ethanol concentration and the air/ethanol mixture is then allowed to flow through the chamber.

With the uncoated and coated SOI MRRs used here, we measure Q values of about 26000 and 15000. Probably, this reduction in quality factor is related to scattering losses due to the imperfections of the drop cast ZnO nanocrystal film. However, a Q value of 15000 still

#126035 - $15.00 USD Received 26 Mar 2010; revised 5 May 2010; accepted 7 May 2010; published 20 May 2010

corresponds to a MRR resonance bandwidth (full width half max) of approximately 100 pm, which is narrow enough to run our sensitivity measurements.

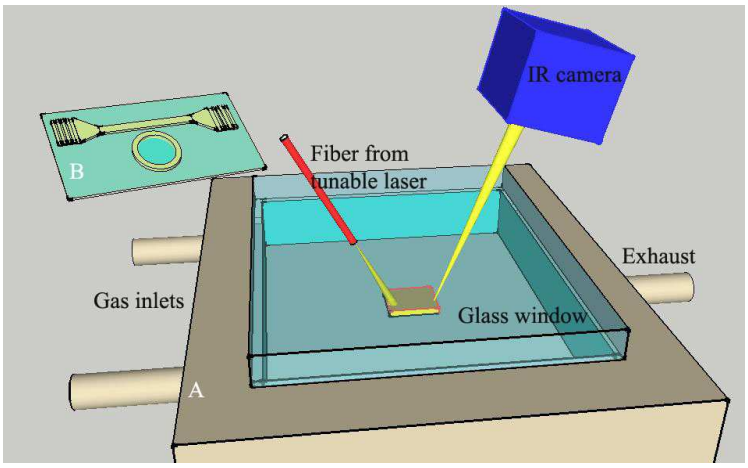

Fig. 3. (a). Schematic representation of the experimental setup; the optical chip containing the MRR ethanol sensor is kept in a gas chamber. A transparent glass window seals the top side of the chamber. Light is coupled in and out of the chip vertically through the window. (b). Schematic view of the MRR with the grating couplers that are used to couple light in and out of the MRR.

Figure 4 represents the experimental results of a typical ethanol sensing experiments. Figure 4(a) shows the measured transmission at the through port of a MRR for different ethanol concentrations c_{EtOH}, expressed in ppm, in air. One sees that exposure to ethanol leads to a redshift of the resonance wavelength. This corresponds to an increase of the effective refractive index upon accumulation of ethanol in the ZnO film. Exposure to 1500 ppm of ethanol leads to a shift of 500 pm. Moreover, one sees that even at 120 ppm of ethanol, a pronounced shift of the resonance wavelength by 220 pm is measured.

The corresponding sensitivity curve is shown in Fig. 4(b), where the markers indicate experimental datapoints and the trend line is a best fit to a Langmuir isotherm. Assuming that $\Delta\lambda$ is proportional to the volume of adsorbed ethanol, and writing the partial pressure p_{EtOH} of ethanol as $c_{\mathrm{EtOH}}/10^6$ bar, this isotherm reads [24]:

$$\Delta\lambda = \Delta\lambda_{\max}\frac{Kp_{\mathrm{EtOH}}}{1+Kp_{\mathrm{EtOH}}} = \Delta\lambda_{\max}\frac{Kc_{\mathrm{EtOH}}}{10^6+Kc_{\mathrm{EtOH}}}. \qquad (5)$$

From the fit, we obtain an equilibrium constant K of about $4(1)\ 10^3$, corresponding to a free energy of adsorption of −20(1) kJ/mol, and a maximum wavelength shift of 560(40) pm. The good correspondence with the Langmuir-model and the relatively low free energy of adsorption suggest that we are looking at the adsorption of a monolayer of ethanol, mainly driven by physisorption [24]. The limiting value of 560 pm for the resonance wavelength shift is in reasonable agreement with the initial rough estimate of 1.2 nm.

#126035 - $15.00 USD Received 26 Mar 2010; revised 5 May 2010; accepted 7 May 2010; published 20 May 2010

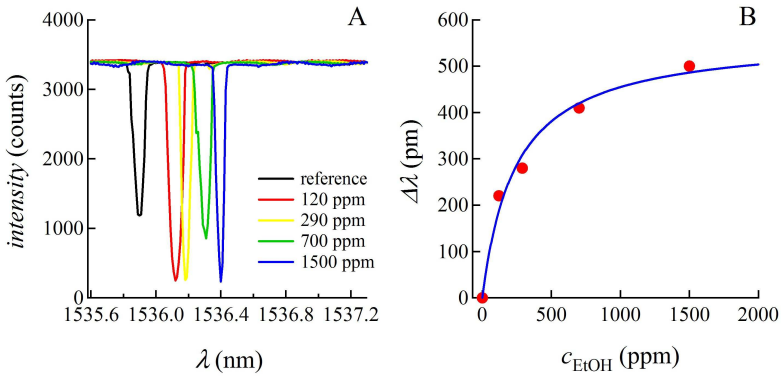

Fig. 4. (a). Measured transmission spectrum of the sensor as a function of ethanol vapor concentration. (b). The corresponding measured resonance shift at different vapor concentrations; the solid curve represents a best fit to a Langmuir isotherm.

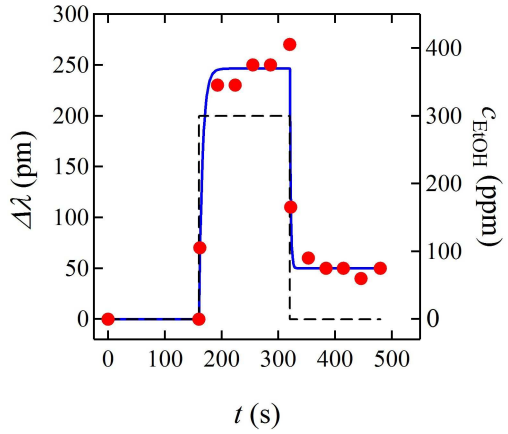

Fig. 5. Temporal response of the sensor for one on-off cycle upon exposure to 300 ppm ethanol. The solid lines are fits of the rising and falling edges of the response to exponentials. The dashed line shows the switching between 0 and 300 ppm ethanol.

For now, 100 ppm is the lowest concentration we can achieve due to the limitations of cooling and the flow capabilities we have at the moment. However, an interpolation of the sensitivity curve using the Langmuir isotherm between 0 and 100 ppm indicates that ethanol concentrations of 25 ppm lead to a shift of 50 pm. As this shift corresponds to the half width at half maximum of the ring resonance, sensing of 25 ppm of ethanol is clearly feasible with this detector.

The sensor response with time at 300 ppm ethanol is shown in Fig. 5, where the markers indicate data points and the trend lines fit to exponentials. We find that the sensor reaches 90% of its near-steady 'on' response within 15 s, while 80% recovery with respect to the pre-ethanol exposure resonance wavelength is achieved within 6 s with adequate air flow (2L/min) in the chamber. Apart from this rapid response, an additional slow and small drift of the sensor is observed after its initial 'on' response, which may be due to ethanol adsorption at poorly accessible surface sites. Since these drifts are as small as 10 to 30 pm, the initial response observed within 2 min is chosen to characterize the sensor. In addition, only a partial recovery of the sensor is achieved within 5 min after the 'off' response. This probably reflects residual ethanol not released from adsorption sites on the ZnO surface. Owing to this fact, the sensor is cleaned with an air flow for at least 10 min after every measurement until it recovers back to the original resonance location.

#126035 - $15.00 USD Received 26 Mar 2010; revised 5 May 2010; accepted 7 May 2010; published 20 May 2010

5. Conclusions

In this work, we have demonstrated the promise of nanocrystalline metal oxide film coated SOI MRRs for low power, compact, reasonably sensitive and low cost integrated optical gas sensing. This demonstrates that metal oxides, which have been extensively used in electrical gas sensors can also be exploited for integrated optical gas sensing. It is shown that ethanol vapor concentrations below 100 ppm can readily be detected with an SOI MRR coated with a nanocrystalline ZnO film. Metal oxides can be doped with molecules selective to different gases. With future advancements in micro-patterning techniques, such selective films can efficiently be coated on several MRRs to achieve integrated and multiplexed multi-gas sensing on an optical chip.

Acknowledgements

The authors acknowledge the Belgian Science Policy (Belspo) for funding through the IAP 6.10 *photonics@be* network. Z.Hens acknowledges the FWO-Vlaanderen for an equipment grant. N. Yebo acknowledges Ghent University for funding this work through the Methusalem project “Smart photonic ICs”.

#126035 - $15.00 USD Received 26 Mar 2010; revised 5 May 2010; accepted 7 May 2010; published 20 May 2010